Calibrating the exchange coefficient in the modified coupled continuum pipe-flow model for flows in karst aquifers

Nan Chen[a], Max Gunzburger[b], Bill Hu[c], Xiaoming Wang[d,*], Celestine Woodruff[e]

[a]*School of Mathematical Sciences, Fudan University, Shanghai, China, 200433. Email: chennan@fudan.edu.cn.*

[b]*Department of Scientific Computing, Florida State University, Tallahassee, FL, 32306-4120. Email: gunzburg@fsu.edu.*

[c]*Department of Earth, Ocean and Atmospheric Science, Florida State University, Tallahassee, FL, 32306-4520. Email: hu@gly.fsu.edu.*

[d]*Department of Mathematics, Florida State University, Tallahassee, FL, 32306-4510. Email: wxm@math.fsu.edu.*

[e]*Department of Mathematics, Florida State University, Tallahassee, FL, 32306-4120. Email: cwoodruf@mail.math.fsu.edu.*

Abstract

We investigate the validity of the popular coupled-continuum pipe-flow (CCPF) model for flow in a karst aquifer. The (Navier) Stokes-Darcy model is used as the "true model" for calibrating the exchange coefficient in the CCPF model by minimizing the relative differences between results from the two models or at least by having those differences being below a prescribed threshold value. We find that although the CCPF model is never in perfect agreement with the Stokes-Darcy model, there is an almost universal choice for a nearly optimal exchange coefficient such that the relative error is below one percent. Our numerics suggest that the nearly optimal choice of the exchange coefficient should be sufficiently large instead of being a small quantity that is

*Corresponding author. Email Address: wxm@math.fsu.edu. Address: 208 James J. Love Building, Department of Mathematics, Florida State University, 1017 Academic Way, Tallahassee, FL, 32306-4510, USA. Tel.: +1 850 644 6419; Fax.: +1 850 644 4053.

proportional to the hydraulic conductivity, as suggested in existing literatures. We also show that this nearly optimal choice of exchange coefficient is robust under a wide range of model parameters. This result demonstrates that the CCPF model is a valid approximation for flows in karst aquifers as long as we set the fluid exchange coefficient sufficiently large and at least in the simple two-dimensional setting that we consider.

Key words: exchange coefficient, coupled-continuum pipe-flow (CCPF) model, Stokes-Darcy model, karst aquifer

1 Introduction

Well developed karst aquifers, in addition to a porous limestone matrix, typically have large cavernous conduits that are known to largely control groundwater flow and contaminant transport within the aquifer (Katz et al. 1998). One of the commonly used approaches to fluid flow in karst aquifers is the coupled continuum pipe-flow model (CCPF) (Bauer et al. 2000, 2003; Birk et al. 2003; Chen et al. 1988; Kiral 1998; MacQuarrie et al. 1996). The CCPF model is a dual flow system consisting of a matrix representing the bulk mass of permeable limestone and a conduit system representing the karst conduit network. Flow exchange between the two systems is controlled by differences in hydraulic heads as well as the hydraulic conductivity and the geometric setting. In the CCPF model, the groundwater flow in the matrix is described by the Darcy's law and the flow in the conduit is modeled by a pipe-flow model. The water mass exchange flow rate between the two systems is described by a first-order mass exchange model; the exchange flow rate is assumed to be linearly proportional to the head difference between the two systems (Barenblatt et al. 1960; Sauter 1992; Teutsch 1989). The exchange rate coefficient, denoted α_{ex}, is a crucial parameter. It is a lumped parameter and its value will depend on many factors including, among others, the hydraulic conductivity in the matrix, the exchange surface between the conduit and matrix, and conduit geometry (Barenblatt et al. 1960; Liedl et al. 2003). The value of the exchange rate parameter is not usually obtained from measurements but rather through curve-fitting. This CCPF model was utilized in studying conduit genesis (Bauer et al. 2000; 2003; Birk et al. 2003; Clemens et al. 1996; Liedl et al. 2003) and is now incorporated in the latest version of the US Geological Survey's popular groundwater software MODFLOW (Shoemaker et al. 2008; Harbaugh 2005) (The conduit flow process part is usually termed CFP).

A major advantage of this approach is its relative simplicity and computational efficiency compared to other models (i.e. the coupled Stokes-Darcy system). Existing literature suggests that α_{ex} should be set to the order of the hydraulic conductivity (Bauer et al. 2000, 2003). Even so, it has been observed that there is high sensitivity of the solution in this regime of the parameter (Bauer et al. 2000, 2003; Birk et al. 2003; Hua 2009; Liedl et al. 2003). Therefore, there is an urgent need to provide guidance on the selection of this critical exchange parameter as well as the validity of the CCPF model. On the other hand, there is an alternative approach for laminar fluid flows in karst aquifers using the coupled Stokes (in the conduit) and Darcy (in the matrix) model (Cao et al. 2010; Discacciati et al. 2002; Faulkner et al. 2009, Layton et al. 2003). The two flow systems are coupled via the empirical Beavers-Joseph interface boundary condition and the model is known to be physically and mathematically sound (Beavers and Joseph 1967; Cao et al. 2010b; Discacciati et al. 2002, Saffman 1971). It has been demonstrated that this model can capture the fluid flow and the transport of contaminants very well in a controlled environment (Faulkner et al. 2009). Therefore, it makes sense for us to assess the validity of CCPF model, assuming that the coupled Stokes-Darcy model is the "true model".

In this work, we address the following **important issues**:

- What is the (near) optimal choice of the fluid exchange coefficient α_{ex} so that the relative error between the solution to the coupled continuum pipe-flow model and the solution of the established coupled Stokes-Darcy model is (essentially) minimized?

- How does the (near) optimal choice of exchange coefficient depend on the system parameters?

- How does the minimum discrepancy (under the near optimal choice of exchange coefficient) between the two models depend on the system parameters?

There are several natural criteria that can be used to measure the discrepancy between the solutions of the two models. These different criteria will be discussed in detail later in section 4.

The problem that we propose to tackle here is a difficult one since it is an optimization problem constrained by partial differential equations (PDEs). In order to make the problem relatively amenable, we will make the following **assumptions**:

1. We consider a conceptual two dimensional domain for a karst aquifer with a straight horizontal conduit imbedded in the middle of a rectangular porous media (or matrix). In the coupled continuum pipe-flow model (CCPF), the conduit will be simplified to a line located at $y = 0, i.e., \Omega_c = (0, L) \times \{y = 0\}$. The matrix domain takes the form of $\Omega_m = (0, L) \times (0, H_m) \cup (0, L) \times (-H_m, 0)$ where $2H_m$ represents the height of the matrix, L is the horizontal length of the conduit and matrix. In the case of Stokes-Darcy model, the conduit domain is $\Omega_c = (0, L) \times (-H_c, H_c)$, and the matrix is $\Omega_m = (0, L) \times (H_c, H_c + H_m) \cup (0, L) \times (-H_m - H_c, -H_c)$

2. We will assume that the matrix is homogeneous and isotropic with constant permeability Π, and hence constant hydraulic conductivity $\mathbb{K} = \frac{\Pi g}{\nu}$, where ν is the kinematic viscosity of the fluid (water) and g is the gravitational acceleration constant.

3. We investigate the laminar flow regime so that the relatively simple Stokes-Darcy model and the laminar CFP model are applicable.

4. We consider constant Neumann type boundary condition (equivalent to constant fixed flux) so that the laminar CCPF model and Stokes-Darcy model can be reduced to systems of ordinary differential equations in terms of the Fourier coefficients in the horizontal direction. (Of course Fourier expansion is not applicable in the original variable but can be used after an appropriate translation of the unknown.)

The linear constant coefficient ODE systems can be reduced to systems of linear algebraic equations in the setting that we have adopted here. The optimization (to minimize the difference between the CCPF model and the Stokes-Darcy model) is then performed on the reduced linear algebraic systems for parameter regime that corresponds to the Wakulla Spring in Florida (Tincaid 2004). Instead of only searching for the optimal exchange coefficient that absolutely minimizes the discrepancy between the two models, we also identify those values of exchange coefficient so that the relative error is less than or equal to one percent (1%). Such an approach is sensible especially in the presence of uncertainties in terms of geometry, hydraulic conductivity, boundary conditions etc. The (near) optimal fluid exchange coefficient α_{ex} depends on the criterion that we use as expected. However, the conventional choice of an order one constant multiply the hydraulic conductivity does not seem to work. Instead, our study suggests a universal near optimal choice of about 25 for the fluid exchange coefficient so that the relative error is below 1% no matter which matching criterion is used. Moreover, this near optimal choice of fluid exchange coefficient is robust with respect to change of parameters up to an order of magnitude (low sensitivity). This gives us strong indication of the validity of the simplified CCPF model provided that we set the fluid exchange coefficient to the near optimal value (25 for instance).

The rest of the paper is organized as follows. We recall the CCPF model and derive its solution formula in section 2. The coupled Stokes-Darcy model is then investigated in Section 3. We calibrate the exchange coefficient in the CCPF model by matching the solutions to the CCPF model and the Stokes-Darcy model numerically in Section 4 under various parameter setting and different matching criterions. We then offer our conclusion in Section 5.

2 CCPF model

2.1 The Model

Instead of utilizing the original CCPF model that is discrete in space (Bauer et al. 2000, 2003), we utilize a modified continuum version (Cao et al. 2011, Hua 2009, Wang 2010). The exchange coefficient in this continuum model differs from that of the original CCPF model by a factor of the length of a typical conduit segment. A heuristic derivation of this continuum model from the original CCPF model, as well as possible pitfalls of this continuum model in three dimension and reasonable fixes, are available in the literature (Wang 2010). We will focus on the two spatial dimension case for simplicity in this work.

2.1.1 The CCPF model

Under the simplifying assumptions on the geometry of the domain and the homogeneity and isotropy of the porous media, the continuum version of coupled continuum pipe flow model for laminar flow takes the form (Cao et al 2011; Hua 2009; Shoemaker et al 2008, Wang 2010)

$$\begin{cases} -\mathcal{K}\Delta\phi_m = -\alpha_{ex}(\phi_m - \phi_c)\delta_{y=0} + S_m & \text{in } \Omega_m \\ -D\dfrac{\partial^2\phi_c}{\partial x^2} = \alpha_{ex}(\phi_m(0) - \phi_c) + S_c & \text{in } \Omega_c \end{cases} \tag{1}$$

where $\Omega_m = (0, L) \times (0, H_m) \cup (0, L) \times (-H_m, 0)$ and $\Omega_c = (0, L) \times \{y = 0\}$ are the regions for the matrix and conduit respectively, $\mathbb{K} = \mathcal{K}\mathbb{I}$ is the hydraulic conductivity tensor (where $\mathcal{K}$ is taken to be a constant under the homogeneous isotropic media assumption), ϕ_m is the hydraulic head in the porous matrix, ϕ_c is the hydraulic head in the conduit, α_{ex} is the fluid exchange coefficient between the matrix and the conduit (the key parameter to be calibrated), $\delta_{y=0}$ is the Dirac delta function concentrated on the conduit $y = 0$, and S_m and S_c are source terms (which will be set to zero in this study). $D = \frac{d^3 g}{12\nu}$, where d is the diameter (or the width in two dimensional case) of the conduit, g is the Earth's gravitational acceleration, ν is the kinematic viscosity of water, and $\phi_m(0)$ represents the restriction of ϕ_m along the line $y = 0$.

The first equation is a consequence of Darcy's equation in the matrix where the second term in the equation models fluid exchange between the conduit and matrix via Barenblatt type approach. The second equation is a consequence of conservation of mass in the conduit where the flow in the conduit is modeled via pipe flow model, and the second term in the equation models fluid exchange.

2.1.2 The boundary conditions

As we mentioned earlier in the introduction, we will postulate the following Neumann boundary condition which is equivalent to specifying the flux at the boundary :

$$\begin{cases} \dfrac{\partial \phi_m}{\partial x}\Big|_{x=0} = f_{ml}, \quad \dfrac{\partial \phi_m}{\partial x}\Big|_{x=L} = f_{mr}, \\ \dfrac{\partial \phi_c}{\partial x}\Big|_{x=0} = f_{cl}, \quad \dfrac{\partial \phi_c}{\partial x}\Big|_{x=L} = f_{cr}, \\ \dfrac{\partial \phi_m}{\partial y}\Big|_{y=\pm H_m} = 0. \end{cases} \tag{2}$$

Due to the incompressibility of the model, we must have the following *compatibility* condition satisfied on the boundary conditions (equivalent to mass conservation):

$$2\mathcal{K}H_m(f_{mr} - f_{ml}) + D(f_{cr} - f_{cl}) = 0. \tag{3}$$

It is easy to observe that the case with prescribed head can be investigated in a similar fashion. However, we will not focus on this part since the Stokes-Darcy system does not seem to enjoy straightforward Fourier expansion in the horizontal direction under prescribed pressure head boundary condition.

2.2 Solution to the CCPF model

2.2.1 Solution strategy

Due to the prescribed constant Neumann boundary condition, we can now define the following two new unknowns

$$\frac{\partial \widetilde{\phi}_m}{\partial x}(x,y) = \frac{\partial \phi_m}{\partial x}(x,y) - (f_{ml} + \frac{x}{L}(f_{mr} - f_{ml})), \tag{4}$$

$$\widetilde{\phi}_c'(x) = \phi_c'(x) - (f_{cl} + \frac{x}{L}(f_{cr} - f_{cl})). \tag{5}$$

It is easy to see that $\frac{\partial \widetilde{\phi}_m}{\partial x}(0,y) = \frac{\partial \widetilde{\phi}_m}{\partial x}(L,y) = 0$ and $\widetilde{\phi}_c'(0) = \widetilde{\phi}_c'(L) = 0$, giving us homogeneous Neumann boundary conditions. Therefore we can employ Fourier cosine expansion in the x variable to reduce the CCPF model Eq. (1) into an infinite system of decoupled ODEs for the Fourier coefficients that we can solve mode by mode.

2.2.2 The CCPF solution formula

Solving the infinite decoupled ODEs for the Fourier coefficients and converting the Fourier mode solution for the translated unknowns back into our original variables, we deduce the following solution formula to the CCPF model:

$$\phi_m(x,y) = f_{ml}x + \frac{1}{2L}(f_{mr} - f_{ml})(x^2 - y^2) + B$$
$$+ \begin{cases} \frac{H_m}{L}(f_{mr} - f_{ml})y + \sum_{k=1}^{\infty} \mathcal{C}_k (e^{\frac{k\pi y}{L}} + e^{\frac{k\pi}{L}(2H_m - y)}) \cos\left(\frac{k\pi x}{L}\right), & y \in (0, H_m) \\ -\frac{H_m}{L}(f_{mr} - f_{ml})y + \sum_{k=1}^{\infty} \mathcal{C}_k (e^{\frac{k\pi}{L}(2H_m + y)} + e^{-\frac{k\pi y}{L}}) \cos\left(\frac{k\pi x}{L}\right), & y \in (-H_m, 0) \end{cases} \tag{6}$$

$$\phi_c(x) = f_{cl}x + \frac{1}{L}(f_{cr} - f_{cl})\left(\frac{x^2}{2} + \frac{D}{\alpha_{ex}}\right) + B + \frac{L}{6}(f_{mr} + 2f_{ml} - f_{cr} - 2f_{cl})$$
$$+ \sum_{k=1}^{\infty} \frac{\alpha_{ex}[\mathcal{C}_k(1 + e^{\frac{2k\pi H_m}{L}}) - \hat{S}_k]}{\alpha_{ex} + \frac{k^2\pi^2}{L^2}D} \cos\left(\frac{k\pi x}{L}\right) \tag{7}$$

where B is an arbitrary constant (head is only determined up to a constant), and the coefficients are given by

$$\mathcal{C}_k = \frac{c_{0,k}L}{2k\pi(1 - e^{\frac{2k\pi H_m}{L}})}, \tag{8}$$

with

$$c_{0,k} = \frac{2\alpha_{ex}D\frac{k^2\pi^2}{L^2}\hat{S}_k(1 - e^{\frac{2k\pi H_m}{L}})}{\alpha_{ex}D\frac{k\pi}{L}(1 + e^{\frac{2k\pi H_m}{L}}) - 2\mathcal{K}(1 - e^{\frac{2k\pi H_m}{L}})(\alpha_{ex} + D\frac{k^2\pi^2}{L^2})} \tag{9}$$

and

$$\hat{S}_k = \frac{2L}{(k\pi)^2}[(f_{ml} - f_{cl}) - (-1)^k(f_{mr} - f_{cr})]. \tag{10}$$

3 The coupled Stokes-Darcy system

3.1 The Stokes-Darcy model

3.1.1 The model

The coupled Stokes-Darcy model for laminar flow in the karst aquifer under consideration takes the form (Beavers and Joseph 1967, Cao et al 2010b, Discacciati et al. 2002, Layton et al. 2003, Nield 1977)

$$\begin{cases} \dfrac{\nu n}{\Pi}\vec{u}_m + n\nabla p_m = -ng\vec{j}, \quad \nabla \cdot \vec{u}_m = 0, \quad \text{in } \Omega_m, \\ -2\nu\nabla \cdot \mathbb{D}(\vec{u}_c) + \nabla p_c = -g\vec{j}, \quad \nabla \cdot \vec{u}_c = 0, \quad \text{in } \Omega_c, \end{cases} \tag{1}$$

where $\vec{j} = (0,1)^T$ denotes the unit vector in (upward) vertical direction, $\Omega_m = (0,L)\times(H_c, H_c+H_m)\cup(0,L)\times(-H_m-H_C, -H_c)$ and $\Omega_c = (0,L)\times(-H_c, H_c)$ are the regions for the matrix and conduit respectively, $\vec{u}_m$, $\vec{u}_c$, p_m and p_c are the velocity and the kinematic pressure in the matrix and conduit respectively, ν denotes the kinematic viscosity, n the porosity, Π the permeability, and $\mathbb{D}(\vec{u}) = \frac{1}{2}\big(\nabla\vec{u}+(\nabla\vec{u})^T\big)$ the deformation rate tensor.

The first equation is the classical Darcy's equation characterizing fluid flow in the matrix while the second equation is the standard Stokes equations governing the motion of fluid in the conduit. Compared to the CCPF model, the flow in the conduit is now modeled via the Stokes equations instead of the simple pipe flow. Moreover, the fluid exchange is no longer explicitly included in the equations but modeled through interface boundary conditions described in the next subsection instead of in an ad-hoc fashion as in the CCPF model.

3.1.2 Boundary and interface conditions

We need to equip the Stokes-Darcy system Eq. (1) with boundary conditions that are compatible with the Neumann boundary condition for the CCPF model Eq. (2). For the pressure in the matrix, we prescribe Neumann boundary condition (equivalent to prescribed flux). For the velocity in the conduit, we utilize the stream function ψ which is related to the velocity through

$$\vec{u}_c = \left(-\frac{\partial \psi}{\partial y}, \frac{\partial \psi}{\partial x}\right) = \nabla^{\perp}\psi. \tag{2}$$

and we will prescribe the value of the stream function ψ at the ends of the conduit ($x = 0, L$) that are compatible with parabolic profile. Therefore we postulate the following boundary conditions.

$$\begin{aligned}
&\frac{\partial p_m}{\partial x}(x,y)\Big|_{x=0} = g \cdot f_{ml}, \quad \frac{\partial p_m}{\partial x}(x,y)\Big|_{x=L} = g \cdot f_{mr},\\
&\frac{\partial p_m}{\partial y}(x,y)\Big|_{y=\pm(H_m+H_c)} = -g,\\
&\psi\Big|_{x=0} = c_l\left(\frac{y^3}{3H_c^2} - y\right), \quad \psi\Big|_{x=L} = c_r\left(\frac{y^3}{3H_c^2} - y\right).
\end{aligned} \tag{3}$$

together with the following classical empirical Beavers-Joseph boundary conditions (Beavers and Joseph 1967)

$$\begin{aligned}
\vec{u}_c \cdot \vec{n}_{mc} &= \vec{u}_m \cdot \vec{n}_{mc},\\
-\vec{n}_{mc} \cdot \big(\mathbb{T}(\vec{u}_c, p_c)\vec{n}_{mc}\big) &= p_m,\\
-\vec{\tau}_{mc} \cdot \big(\mathbb{T}(\vec{u}_c, p_c)\vec{n}_{mc}\big) &= \alpha_{BJ}\tfrac{\nu}{\sqrt{\Pi}}\vec{\tau}_{mc} \cdot (\vec{u}_c - \vec{u}_m),
\end{aligned} \tag{4}$$

where α_{BJ} is an empirical constant determined by the geometry and the material (will be set to $\alpha_{BJ} = 1$ for simplicity in this study), $\vec{n}_{mc}$ is the unit outer normal to the matrix at the interface, and $\vec{\tau}_{mc} = (1, 0)$ is the (positive) unit tangent vector to the interface.

The boundary conditions on the pressure in porous media in Equation (3) are consistent with the boundary condition on the head in the porous media for the CCPF model in Equation (2) since

$$h_m = \frac{p_m}{g} + y. \tag{5}$$

The prescribed boundary value for the stream-function in Equation (3) implies that the horizontal velocity in the conduit enjoys the following parabolic profile

$$u_{c,1}\big|_{x=0} = v_l(y) := -c_l\left(\frac{y^2}{H_c^2} - 1\right), \quad u_{c,1}\big|_{x=r} = v_r(y) := -c_r\left(\frac{y^2}{H_c^2} - 1\right). \tag{6}$$

The constants in the parabolic profiles for flow in the conduit must be taken in the following manner so that they are consistent with the specified discharge (flux) for the CCPF model Eq. (2)

$$f_{cr} = \frac{-4c_r H_c}{3D}, \quad f_{cl} = \frac{-4c_l H_c}{3D}. \tag{7}$$

The mass conservation then dictates

$$f_{mr} - f_{ml} = \frac{-2(c_l - c_r)H_c}{3\mathcal{K}H_m} \tag{8}$$

which is equivalent to Equation (3).

It is worthwhile to point out that the case with prescribed head can be considered as well in principle. However the Fourier methodology may not be applicable. For instance, fixed head implies Fourier sine expansion (after appropriate translation) for the pressure in the conduit while parabolic profile also suggests Fourier sine expansion (after appropriate translation) for the horizontal velocity in the conduit, and these two sine expansions are not consistent with the Stokes equations (1). It should be noted that the horizontal (x) derivative of the stream function should be specified at the ends of the conduit ($x = 0, L$) as well in order to specify the whole velocity. This is implicitly done here by the incompressible condition and the assumption that the translated stream-function (10) enjoys sine expansion in the x direction in both L^2 and H^1 space (hence the translated vertical velocity satisfies homogeneous Neumann boundary at condition at the ends of the conduit).

3.2 Solution to the Stokes-Darcy system

3.2.1 Solution strategy

For the Darcy part, we use the pressure p_m as the main (prognostic) variable which satisfies the Laplace equation. Introducing the following translated new unknown

$$\widetilde{p}_m = p_m - g\left[x \cdot f_{ml} + \frac{x^2}{2L}(f_{mr} - f_{ml})\right], \tag{9}$$

which is equipped with homogeneous Neumann boundary condition $\frac{\partial \widetilde{p}_m}{\partial x}(0, y) = 0 = \frac{\partial \widetilde{p}_m}{\partial x}(L, y)$. Therefore we could employ Fourier cosine expansion in the x variable for $\tilde{p}_m$.

As for the Stokes part, we work with the stream-function ψ which satisfies the bi-harmonic equation $\Delta^2\psi = 0$. In order to homogenize the boundary conditions at the lateral ends, we introduce the following translated stream-function

$$\widetilde{\psi}(x, y) = \psi(x, y) + \int_0^y \left[v_l(s) + \frac{x}{L}(v_r(s) - v_l(s))\right] ds. \tag{10}$$

This translated stream-function is zero (homogeneous Dirichlet boundary condition) at the lateral ends ($x = 0, L$). Hence, the translated velocity $\tilde{\vec{u}}_c = \nabla^{\perp}\tilde{\psi}$ satisfies the homogenous Dirichlet boundary condition for the horizontal velocity $\widetilde{u}_{c,1}$, and homogeneous Neumann boundary condition for the translated vertical velocity $\widetilde{u}_{c,2}$ at the lateral ends. Therefore we could employ Fourier sine expansion in x for the translated horizontal velocity and the stream function, and Fourier cosine expansion in x for the translated vertical velocity and pressure in the conduit.

3.2.2 Solution formula for the Stokes-Darcy model

Solving the resulting infinitely many decoupled constant coefficient ODEs for the Fourier coefficients and revert back to the original variable, we deduce the following solution formula for the Stokes-Darcy system Eq. (1) together with the boundary conditions Eq. (3) and interface conditions Eq. (4).

The head in the matrix is given by

$$h_m(x,y) = f_{ml}x + \frac{1}{2L}(f_{mr}-f_{ml})(x^2-y^2) + B' + \begin{cases} \dfrac{H_m+H_c}{L}(f_{mr}-f_{ml})y + \dfrac{1}{g}\displaystyle\sum_{k=1}^{\infty}(C_5 e^{\frac{k\pi y}{L}} + C_6 e^{-\frac{k\pi y}{L}})\cos\left(\frac{k\pi x}{L}\right), & y > H_c \\ -\dfrac{H_m+H_c}{L}(f_{mr}-f_{ml})y + \dfrac{1}{g}\displaystyle\sum_{k=1}^{\infty}(C_7 e^{\frac{k\pi y}{L}} + C_8 e^{-\frac{k\pi y}{L}})\cos\left(\frac{k\pi x}{L}\right), & y < -H_c, \end{cases} \tag{11}$$

and the velocity in the conduit is given by

$$\begin{aligned} u_{c,1}(x,y) &= v_l(y) + \frac{x}{L}(v_r(y)-v_l(y)) + \sum_{k=1}^{\infty}\Bigg[-\frac{k\pi}{L}C_1 e^{\frac{k\pi y}{L}} + \frac{k\pi}{L}C_2 e^{-\frac{k\pi y}{L}} \\ &\qquad - \left(1+\frac{k\pi y}{L}\right)C_3 e^{\frac{k\pi y}{L}} - \left(1-\frac{k\pi y}{L}\right)C_4 e^{-\frac{k\pi y}{L}}\Bigg]\sin\left(\frac{k\pi x}{L}\right) \\ u_{c,2}(x,y) &= -\frac{1}{L}\int_0^y (v_r(s)-v_l(s))ds + \sum_{k=1}^{\infty}\Bigg[\frac{k\pi}{L}C_1 e^{\frac{k\pi y}{L}} + \frac{k\pi}{L}C_2 e^{-\frac{k\pi y}{L}} \\ &\qquad + \frac{k\pi}{L}C_3 y e^{\frac{k\pi y}{L}} + \frac{k\pi}{L}C_4 y e^{-\frac{k\pi y}{L}}\Bigg]\cos\left(\frac{k\pi x}{L}\right) \end{aligned} \tag{12}$$

where the coefficients C_1–C_8 are determined via solving the following systems of linear algebraic equations:

$$e^{\frac{k\pi(H_m+H_c)}{L}}C_5 - e^{-\frac{k\pi(H_m+H_c)}{L}}C_6 = 0 \tag{C1}$$

$$e^{-\frac{k\pi(H_m+H_c)}{L}}C_7 - e^{\frac{k\pi(H_m+H_c)}{L}}C_8 = 0 \tag{C2}$$

$$e^{\frac{k\pi H_c}{L}}C_1 + e^{-\frac{k\pi H_c}{L}}C_2 + H_c\left(e^{\frac{k\pi H_c}{L}}C_3 + e^{-\frac{k\pi H_c}{L}}C_4\right) + \frac{\Pi}{\nu}\left(e^{\frac{k\pi H_c}{L}}C_5 - e^{-\frac{k\pi H_c}{L}}C_6\right) = 0 \tag{C3}$$

$$2\nu\left(\frac{k\pi}{L}\right)^2\left[-C_1 e^{\frac{k\pi H_c}{L}}+C_2 e^{-\frac{k\pi H_c}{L}}-H_c\left(C_3 e^{\frac{k\pi H_c}{L}}-C_4 e^{-\frac{k\pi H_c}{L}}\right)\right]-C_5 e^{\frac{k\pi H_c}{L}}-C_6 e^{-\frac{k\pi H_c}{L}}$$
$$=\widehat{P}_{m,k}(H_c)-\frac{2\nu k\pi}{L}\widehat{F}_{c,1,k}(H_c)+\frac{L\nu}{k\pi}\widehat{F}''_{c,1,k}(H_c) \quad \text{(C4)}$$

$$\left(2\left(\frac{k\pi}{L}\right)^2+\frac{k\pi\alpha_{BJ}}{L\sqrt{\Pi}}\right)e^{\frac{k\pi H_c}{L}}C_1+\left(2\left(\frac{k\pi}{L}\right)^2-\frac{k\pi\alpha_{BJ}}{L\sqrt{\Pi}}\right)e^{-\frac{k\pi H_c}{L}}C_2$$
$$+\left(2\frac{k\pi}{L}+\frac{\alpha_{BJ}}{\sqrt{\Pi}}\right)\left(1+\frac{k\pi H_c}{L}\right)e^{\frac{k\pi H_c}{L}}C_3+\left(-2\frac{k\pi}{L}+\frac{\alpha_{BJ}}{\sqrt{\Pi}}\right)\left(1-\frac{k\pi H_c}{L}\right)e^{-\frac{k\pi H_c}{L}}C_4$$
$$+\frac{k\pi\alpha_{BJ}\sqrt{\Pi}}{L\nu}\left(e^{\frac{k\pi H_c}{L}}C_5+e^{-\frac{k\pi H_c}{L}}C_6\right)=\widehat{F}'_{c,1,k}(H_c)+\frac{\alpha_{BJ}}{\sqrt{\Pi}}\left(\widehat{F}_{c,1,k}(H_c)+\frac{\Pi}{\nu}\widehat{F}_{m,1,k}(H_c)\right)$$
$$\text{(C5)}$$

$$e^{-\frac{k\pi H_c}{L}}C_1+e^{\frac{k\pi H_c}{L}}C_2-H_c\left(e^{-\frac{k\pi H_c}{L}}C_3+e^{\frac{k\pi H_c}{L}}C_4\right)+\frac{\Pi}{\nu}\left(e^{-\frac{k\pi H_c}{L}}C_7-e^{\frac{k\pi H_c}{L}}C_8\right)=0$$
$$\text{(C6)}$$

$$2\nu\left(\frac{k\pi}{L}\right)^2\left[-e^{-\frac{k\pi H_c}{L}}C_1+e^{\frac{k\pi H_c}{L}}C_2+H_c\left(e^{-\frac{k\pi H_c}{L}}C_3-e^{\frac{k\pi H_c}{L}}C_4\right)\right]-e^{-\frac{k\pi H_c}{L}}C_7-e^{\frac{k\pi H_c}{L}}C_8$$
$$=\widehat{P}_{m,k}(-H_c)-\frac{2\nu k\pi}{L}\widehat{F}_{c,1,k}(-H_c)+\frac{L\nu}{k\pi}\widehat{F}''_{c,1,k}(-H_c) \quad \text{(C7)}$$

$$\left(-2\left(\frac{k\pi}{L}\right)^2+\frac{k\pi\alpha_{BJ}\nu}{L\sqrt{\Pi}}\right)e^{-\frac{k\pi H_c}{L}}C_1-\left(2\left(\frac{k\pi}{L}\right)^2+\frac{k\pi\alpha_{BJ}\nu}{L\sqrt{\Pi}}\right)e^{\frac{k\pi H_c}{L}}C_2$$
$$+\left(-2\frac{k\pi}{L}+\frac{\alpha_{BJ}\nu}{\sqrt{\Pi}}\right)\left(1-\frac{k\pi H_c}{L}\right)e^{-\frac{k\pi H_c}{L}}C_3+\left(2\frac{k\pi}{L}+\frac{\alpha_{BJ}\nu}{\sqrt{\Pi}}\right)\left(1+\frac{k\pi H_c}{L}\right)e^{\frac{k\pi H_c}{L}}C_4$$
$$+\frac{k\pi\alpha_{BJ}\sqrt{\Pi}}{L}\left(e^{-\frac{k\pi H_c}{L}}C_7+e^{\frac{k\pi H_c}{L}}C_8\right)=-\widehat{F}'_{c,1,k}(-H_c)+\frac{\alpha_{BJ}\nu}{\sqrt{\Pi}}\left(\widehat{F}_{c,1,k}(-H_c)+\frac{\Pi}{\nu}\widehat{F}_{m,1,k}(-H_c)\right) \tag{C8}$$

and

$$\begin{aligned}&\widehat{F}_{m,1,k}(y)=\frac{2g}{k\pi}\left[f_{ml}-(-1)^k f_{mr}\right] \qquad \text{for } k\neq 0,\\ &\widehat{F}_{m,2,0}(y)=g,\end{aligned} \tag{13}$$

$$\begin{aligned}\widehat{F}_{c,1,k}(y)&=\frac{2}{k\pi}\left[(1-(-1)^k)v_l(y)-(-1)^k(v_r(y)-v_l(y))\right],\\ \widehat{F}_{c,2,0}(y)&=-\frac{1}{L}\int_0^y(v_r(s)-v_l(s))ds.\end{aligned} \tag{14}$$

The constant B' should be set in the following way so that head difference between the Stokes-Darcy system and the CCPF model can be minimized:

$$B'=B-\frac{H_c}{L}(f_{mr}-f_{ml})\left(H_m+\frac{H_c}{2}\right). \tag{15}$$

It is observed that the above linear algebraic system for the coefficients C_1-C_8 could be very stiff for large k. However, this stiffness is much easier to handle than the stiffness matrix associated with direct numerical discretization.

4 Calibration results

Here we calibrate the fluid exchange coefficient α_{ex} by matching the solution to the CCPF model to that of the Stokes-Darcy model based on the solution formulas presented in the previous two sections. We used 1000 modes in the horizontal direction (truncation wave number in k) for our numerical calculation. The 1000 modes contains more than 99% of the energy of all solutions.

4.1 Criterions

There are several criterions that can be used to calibrate the (near) optimal choice of the fluid exchange coefficient α_{ex} as we mentioned earlier in the introduction. The criterions (in the L^2 norm) that can be used are

1. head on the interface, i.e., $\sqrt{\int_0^L |\phi_m(x,0) - h_m(x,H_c)|^2\,dx}$;
2. the normal velocity on the interface which is equivalent to fluid exchange rate between the conduit and the matrix, i.e., $\mathcal{K}\sqrt{\int_0^L (\frac{\partial \phi_m(x,y)}{\partial y}\big|_{y=0} - \frac{\partial h_m(x,y)}{\partial y}\big|_{y=H_c})^2\,dx}$;
3. the head in the matrix, i.e., $\sqrt{\int_0^{H_m}\int_0^L |\phi_m(x,y) - h_m(x,y+H_c)|^2\,dx\,dy}$;
4. the velocity in the matrix, i.e., $\mathcal{K}\sqrt{\int_0^{H_m}\int_0^L |\nabla\phi_m(x,y) - \nabla h_m(x,y+H_c)|^2\,dx\,dy}$; and
5. the discharge in the conduit, i.e., $\sqrt{\int_0^L |-D\phi_c'(x) - \int_{-H_c}^{H_c} u_{c,1}(x,y)\,dy|^2\,dx}$.

As we will see below that the optimal fluid exchange coefficient depends on the choice of the matching criterion used. Fortunately, it seems that there is some kind of universality in the sense that an order one choice for the exchange coefficient works for all criterions reasonably well.

4.2 Wakulla Spring Parameters

We have performed numerical experiments on a set of data corresponding the Wakulla Spring in Florida. Additional numerical experiments on a data set corresponding to a laboratory set-up investigated earlier (Faulkner et al. 2009) have been performed with very much the same result and hence will not be reported here for the sake of brevity.

We chose parameters for our numerical experiments based on a real life example: Wakulla Spring. Wakulla Spring, located near Tallahassee, Florida, is one of the largest and deepest freshwater springs in the world. The parameters (together with their units) used in the numerics for a flood season are summarized below: Horizontal aquifer length (m) $L = 32000$; Height of the matrix (m) $H_m = 100$; Half the height of the conduit (m) $H_c = 2$; Conduit inflow velocity at $y = 0$ (m/s) $c_l = 0.33H_c^2$; Conduit outflow velocity at $y = 0$ (m/s) $c_r = 0.32H_c^2$ ($c_l > c_r$ and hence a flood season); Gravity acceleration constant (m/s^2) $g = 9.8$; Kinematic viscosity for water (m^2/s) $\nu = 10^{-6}$; Height of conduit (m) $d = 2H_c$ (this implies that the constant D in the CCPF model is given by: $D = \frac{gd^3}{12\nu}$ and the unit is (m^2/s)); Permeability (m^2) $\Pi = \frac{350\times10^{-6}}{3600\times24g}$; Hydraulic Conductivity (m/s) $\mathcal{K} = \frac{\Pi g}{\nu}$; Normal derivative of head in the matrix on the left lateral boundary (m/s) $f_{ml} = -5\times10^{-4}\mathcal{K}^{-1}$; Normal derivative of head in the conduit on the right end (m/s) $f_{cr} = \frac{-4c_rH_c}{3D}$; Normal derivative of head in the conduit on the left end (m/s) $f_{cl} = \frac{-4c_lH_c}{3D}$; Normal derivative of head in the matrix on the right lateral boundary (m/s) $f_{mr} = \frac{-2(c_l-c_r)H_c}{3\mathcal{K}H_m} + f_{ml}$; CCPF constant (m) $B = -\frac{L}{3}f_{ml} - \frac{L}{6}f_{mr}$ (this is chosen so that the relative error in head can be big); Stokes-Darcy constant (m) $B' = B - \frac{H_c}{L}(f_{mr} - f_{ml})\left(H_m + \frac{H_c}{2}\right)$; Beavers-Joseph constant (m) $\alpha_{BJ} = 1$.

4.3 Numerical results

The results show the relative error of the root-mean-square (L^2-norm) of the difference of the solutions derived via the two models, instead of the L^2-norm itself. The relative error is computed assuming that the Stokes-Darcy model is the true one. These results are computed only up to the 1000^{th} Fourier mode for the Wakulla Springs data. These 1000 Fourier modes contain more than 99% of the energy (L^2-norm) of all solutions involved.

We first tested the conventional wisdom by setting the exchange coefficient α_{ex} to be exactly the hydraulic conductivity $\mathcal{K}$ (Bauer et al. 2000, 2003, Shoemaker et al. 2008). The relative error in terms of head difference on the interface is an unacceptable 5000% although the relative error in other measures are much less (4.2% in terms of the normal velocity on the interface, 4.7% in terms of the head difference in the porous media, and 0.6% in terms of the discharge in the conduit). Moreover, there exists high sensitivity on α_{ex} in this regime of the parameter as observed earlier in the literature (Bauer et al. 2000, 2003; Birk et al. 2003; Hua 2009; Liedl et al. 2003).

Next, we tested two extreme cases with $\alpha_{ex} = 0$ and the limit of $\alpha_{ex} \to \infty$. In both cases we discovered that the relative error is nonzero which gives us confidence that we can focus on intermediate values for α_{ex}.

It is observed that the relative error never vanishes for the cases that we tested (see for instance Figure 2). This implies that the CCPF model is never a perfect match of the Stokes-Darcy model. We also observed that there may not be a finite value of α_{ex} that minimizes the relative error. (Our numerics with very large wave number k may not be very reliable due to the stiffness of the linear algebraic system for the coefficients $C_1 - C_8$.) However, our numerics demonstrate that there is a threshold value beyond which the relative error is always below 1% for instance. This threshold value of the exchange coefficient will be viewed as near optimal choice. The solid curves in Figure 1 describe relative error as a function of α_{ex} based on either comparing the discharge in the conduit (bottom right panel), or the normal velocity at the interface (top left panel), or head in the matrix (top middle panel), or velocity in the matrix, (bottom left), or head at the interface (top right). The dotted horizontal line is the line with 1% relative error. Our numerics indicate that the relative error will be below the threshold value of 1% provided that $\alpha_{ex} \geq 22$ for the case of comparing head on the interface, the normal velocity on the interface criterion requires $\alpha_{ex} \geq 0.02$, the head in the porous media criterion requires $\alpha_{ex} \geq 0.02$, the velocity in the matrix criterion requires $\alpha_{ex} \geq 0.03$, and the discharge in the conduit criterion leads to the constraint $\alpha_{ex} \geq 3.0 \times 10^{-7}$ with the same threshold level of relative error. Table 1 lists the threshold values of α_{ex} with difference threshold levels of relative error using various criterions.

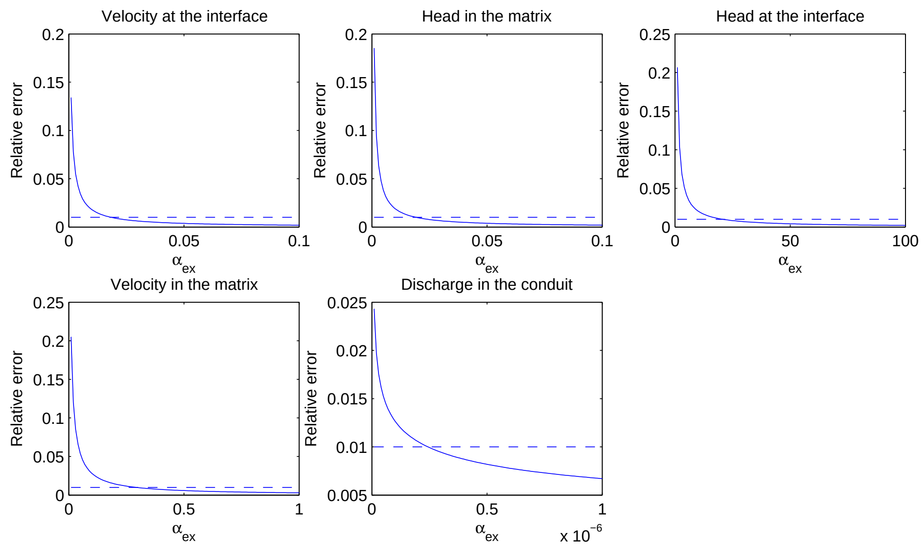

Figure 1: Graphs of the relative errors in the L^2-norm under different criterions. Each panel shows the critical α_{ex} value needed to ensure the relative error to be less than or equal to 1%.

With the uncertainty concerning the geometry as well as the geological parameters associated with the model in mind, we naturally inquire if the numerical results that we obtained on the (near) optimal choice of fluid exchange coefficient α_{ex} are robust under perturbation in the geometry and/or geological parameters. Figure 2 shows the relative error when using normal velocity at the interface as our criterion, given different values of several parameters (top left panel: flux in the conduit; top right panel: conduit radius; middle left panel: half conduit height; middle right panel: permeability; bottom: viscosity). We can observe that an order one choice of α_{ex} will guarantee that the relative error is at most 1%. Figure 3 describes the dependence of the threshold value of α_{ex} corresponding to the 1% relative error and variation of parameters (top left panel: flux in the conduit; top right panel: conduit radius; middle left panel: half matrix height; middle right panel: permeability; bottom panel: viscosity) using normal velocity at the interface as criterion.

Extensive numerical tests covering a drought season for the Wakulla Springs

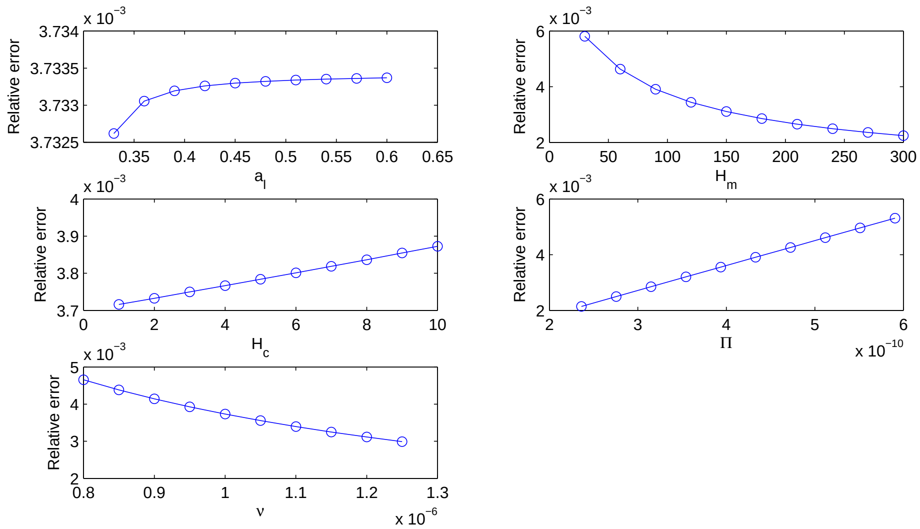

Figure 2: Graphs of the relative error using the optimal α_{ex} and varying other parameters.

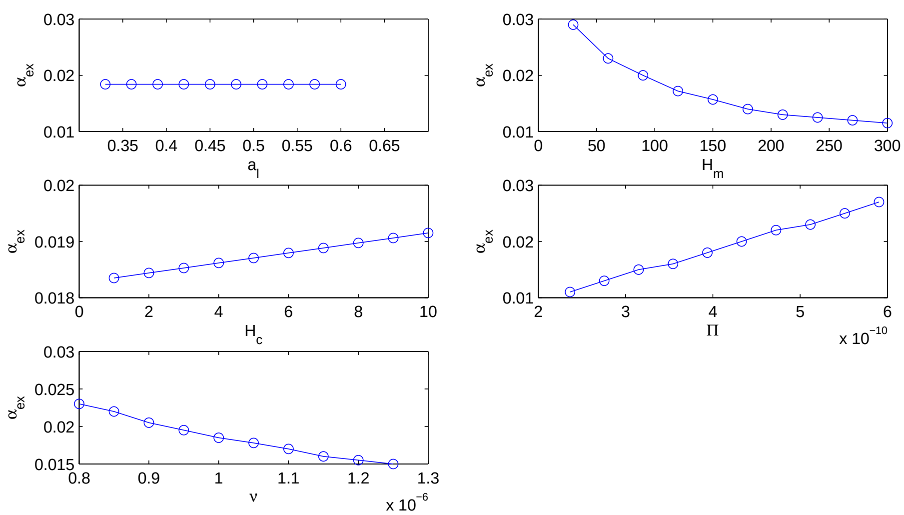

Figure 3: Graphs of the optimal α_{ex} based on the variation of other parameters. Using this range of α_{ex}, the relative error will remain under 1%.

set-up, flood and drought season for a lab set-up (Faulkner et al. 2009), as well as numerous sensitivity tests including sensitivity on the truncation wave number and the Beavers-Joseph coefficient (Beavers and Joseph 1967) within the Stokes-Darcy model have been conducted. All the numerical results are consistent with the results presented here.

5 Conclusion

We have conducted extensive numerical experiments on calibrating the optimal fluid exchange coefficient in the CCPF model Eq. (1) assuming the Stokes-Darcy system Eq. (1) as the "true model". Our numerics demonstrate that

1. The CCPF model is never a perfect match of the Stokes-Darcy model no matter how we choose the exchange coefficient α_{ex}.

2. The conventional wisdom of setting α_{ex} to be of the order of the hydraulic conductivity may lead to large (up to 5000%) relative error depending on the criterions used. Moreover, there exists high sensitivity in this regime of the exchange coefficient.

3. It seems that there exists a natural and universal choice for the fluid exchange coefficient α_{ex} within the CCPF model Eq. (1) that makes the relative error small. Indeed, we can set the α_{ex} sufficiently large (say $\alpha_{ex} = 25$) and obtain an upper bound on the relative error (1%). These results are robust under perturbation on parameters as well as in truncation wave numbers in our numerics. Therefore, the evidences that we have accumulated strongly suggest that the CCPF model is an effective simplified model for laminar flow in karst aquifer as long as we choose the fluid exchange coefficient appropriately (at least 25).

Table 1: Threshold values of α_{ex} (i.e. the smallest value that alpha can have) to ensure desired bounds on the listed relative error.

Criterion	**5%**	**1%**
Comparing the hydraulic head in the matrix	0.004	0.020
Comparing the hydraulic head at the interface	4.2	22
Comparing the normal velocity at the interface	0.004	0.020
Comparing the total discharge in the conduit	3.0×10^{-9}	3.0×10^{-7}

Acknowledgment

This work is supported in part by grants from the NSF through DMS0620035 (CMG grant for MG, BH and XW) and DMS1008852 (XW and CW), a COFRS award from FSU (XW), and an award from the Chinese Ministry of Education for the Modern Applied Mathematics 111 project in Fudan University (NC and XW).

References

1. Barenblatt G., Zheltov I., Kochina I., 1960. Basic concepts in the theory of seepage of homogeneous liquids in fissured rocks. J. Appl. Math. Mech. (USSR), 24, 1286–1303.

2. Bauer S., Liedl R., Sauter M., 2000. Modeling of karst development considering conduit-matrix exchange flow, Calibration and reliability in groundwater modeling: coping with uncertainty. Int Assoc of Hydrol Sci 265:10–15.

3. Bauer S., Liedl R., Sauter M., 2003. Modeling of karst aquifer genesis: Influence of exchange flow. Water Resour Res. Doi:10.1029/2003WR002218.

4. Beavers G., Joseph D. D., 1967. Boundary conditions at a naturally permeable wall. J Fluid Mech 30:197–207.

5. Birk S., Liedl R., Sauter M., Teutsch G., 2003. Hydraulic boundary conditions as a controlling factor in karst genesis. Water Resour. Res., 39, 1004.

6. Cao Y., Gunzburger M., Hua F., Wang X., 2010. Coupled Stokes-Darcy model with Beavers-Joseph interface boundary condition. Commun in Math Sci 8:1–25.

7. Cao Y., Gunzburger M., Hua F., Wang X., 2011. Analysis and finite element approximation of a coupled, continuum pipe-flow/Darcy model for flow in

porous media with embedded conduits. Numer Methods for Partial Differ Equ. vol. 27, no.5., 1242-1252.

8. Chen Y., Bian J., 1988. The media and movement of karst water, in Karst Hydrogeology and Karst Environment Protection: 21st Congress of the International Association of Hydrogeologists, Guilin, China, Int. Assoc. of Hydrogeologists.

9. Clemens T., Hŭckinghaus D., Sauter M., Liedl R., Teutsch G., 1996. A combined continuum and discrete network reactive transport model for the simulation of karst development. IAHS Publ., 237, 309–318.

10. Dershovitz W., Wallmann P., Kindred S., 1991. Discrete fracture network modeling for the Stripa site characterization and validation drift in flow predictions. SKB Stripa Technical Teport TR-91-16, Swed. Nucl. Power and Waste Manage. Co., Stockholm.

11. Discacciati M., Miglio E., Quarteroni A., 2002. Mathematical and numerical models for coupling surface and groundwater flows, *Appl. Num. Math., 43*, 57–74.

12. Faulkner J., Hu B., Kish S., Hua F., 2009. Laboratory analog and numerical study of groundwater flow and solute transport in a karst aquifer with conduit and matrix domains. J of Contam Hydrol 110:34–44.

13. Ford D., 1998. Perspectives in karst hydrology and cavern genesis. Bull. Hydrogeol., 16, 9–29.

14. Ford D., Williams P., 1989. Karst Geomorphology and Hydrology, Chapman and Hall, New York.

15. Harbaugh A., 2005. MODFLOW-2005, the U.S. geological survey modular ground-water model – The ground-water flow process. U.S. Geol Surv Tech

and Methods 6:A16.

16. Hua, F., 2009. Modeling, Analysis and Simulation of Stokes-Darcy System with Beavers-Joseph Interface Condition: PhD, Florida State University, USA.

17. Katz B., Catches J., Bullen T., Michel R., 1998. Changes in the isotopic and chemical composition of ground water resulting from a recharge pulse from a sinking stream. J. Hydrol.; 211, 178–207.

18. Kincaid T., 2004. Exploring the secrets of Wakulla Springs, open seminar, Tallahassee, FL.

19. Kiraly L., 1998. Modeling karst aquifers by the combined discrete channel and continuum approach. Bull. Hydrogeol., 16, 77–98.

20. Kuniansky E., 2008. U.S. Geological Survey Karst Interest Group Proceedings, U.S. Geological Survey Scientific Investigations Report 2008-5023, Bowling Green, 2008.

21. Layton W.J., Schieweck W., Yotov I., 2003. Coupling fluid flow with porous media flow, SIAM J. Num. Anal., **40**, 2195-2218.

22. Liedl R., Sauter M., Hückinghaus D., Clemens T., Teutsch G., 2003. Simulation of the development of karst aquifers using a coupled continuum pipe flow model. Water Resour. Res., 39, 1057.

23. MacQuarrie K., Sudicky E., 1996. On the incorporation of drains into three-dimensional variably saturated groundwater flow models, Water Resour. Res., 32, 447–482.

24. Nield D.A., 1977. Onset of convection in a fluid layer overlying a layer of a porous media. J. Fluid Mech., 81: 513-522.

25. Saffman P., 1971. On the boundary condition at the interface of a porous medium, Stud. in Appl. Math., **1**, 77-84.

26. Sauter M., 1992. Quantification and forecasting of regional groundwater flow and transport in a karst aquifer (Gal lusquel le, Malm SW Germany), Ph.D. Thesis, Univ. of Tübingen, Tübinger, Germany.

27. Shoemaker, W. B., Kuniansky E.L., Birk S., Bauer S., Swain E.D., 2008. Documentation of a conduit flow process (CFP) for MODFLOW-2005, U.S. Geological Survey Techniques and method book 6, Chapter A, Reston, Virginia.

28. Taylor C., Greene E., 2001. Quantitative Approaches in Characterizing Karst Aquifers: U.S. Geological Survey Karst Interest Group Proceedings. Water Resources Investigations Report, 01-4011, 164–166.

29. Teutsch G., 1989. Two practical examples from the Swabian Alb, S. Germany, in Proc. 4th Conference on Solving Groundwater Problems with Models, Indianapolis, 1989.

30. Wang X., 2010. On the coupled continuum pipe flow model (CCPF) for flows in karst aquifer. Discret and Contin Dyn Syst-Ser B 13:489-501.